Effects of Typical Alkaline Earth Metal Salts on Cellulose Torrefaction: Solid Products and Thermal Gravimetric Analysis

Hongfang Zhou,[a] Liang Zhao,[a,]* Xin Fu,[a] Yifeng Zhu,[a] and Yadi Pan [a,b]

To investigate the influencing mechanisms of calcium and magnesium on the solid products of biomass torrefaction, cellulose was selected as the feedstock in this article. The experiments were conducted in the holding temperature range of 200 °C to 300 °C under the atmosphere of nitrogen. Based on the impregnation methods (chlorides, hydroxides, and acetates of Ca and Mg), the results showed that the solid product yield of torrefacted cellulose impregnated with calcium or magnesium salts was lower than that of raw cellulose torrefaction at 200 °C to 275 °C. However, at 300 °C, the solid product yield of impregnated cellulose torrefaction was higher. During torrefaction, the $CaCl_2$ had a stronger effect than other calcium salts. The $Mg(CH_3COO)_2$ had less of an effect than other magnesium salts. The crystallinity of the torrefied cellulose with impregnated calcium or magnesium salts was considerably reduced from 51.1% (raw cellulose) to 7.7% (addition of $CaCl_2$), 34.8% (addition of $Ca(OH)_2$), 28.6% (addition of $Ca(CH_3COO)_2$), 9.2% (addition of $MgCl_2$), 13.6% (addition of $Mg(OH)_2$), and 12.0% (addition of $Mg(CH_3COO)_2$). The results of the thermal gravimetric analysis showed that the impregnated calcium or magnesium salts dramatically reduced the activation energy of the torrefaction.

Keywords: Calcium and magnesium salts; Solid products; Cellulose; Torrefaction; Kinetics

*Contact information: a: College of Materials Science and Engineering, Nanjing Forestry University, Nanjing 210037, China; b: Co-Innovation Center of Efficient Processing and Utilization of Forest Resources, Nanjing Forestry University, Nanjing 210037, China; *Corresponding author: zl_06@126.com*

INTRODUCTION

Among various renewable energy sources, biomass is the only carbon-based source of energy that meets the requirements of replacing fossil fuels to reduce greenhouse gas emissions (Saidur *et al.* 2011; Liu *et al*. 2019). There are three major components in biomass, cellulose, hemicellulose, and lignin. Commonly, cellulose, hemicellulose, and lignin in biomass can reach 40 to 60 wt%, 15 to 30 wt%, and 10 to 25 wt%, respectively (Wang *et al.* 2017a; Huang *et al*. 2019), depending on the biomass species (Zhao *et al.* 2017). In this article, cellulose, the largest quantity in biomass, was used as the feedstock in the experiments. Many kinds of biomass conversion technologies have been developed in recent years, which mainly include thermochemical and biochemical methods. Thermochemical methods, such as torrefaction, are considered to be a central topic in biomass utilization fields (Mohan *et al.* 2006). Torrefaction is a thermal pretreatment process in which biomass is heated under anaerobic or hypoxic conditions at a temperature of 200 ℃ to 300 ℃, with a residence time of less than 1 h, and a heating rate of less than 50 ℃/min (Rousset *et al.* 2013). Compared with raw biomass, the hydrophobicity, grindability, volatile content, calorific value, and combustion characteristic of torrefied biomass are noticeably enhanced (Chen *et al.* 2014). Torrefied cellulose could reduce the O/C ratio and increase crystallinity and heating value (Wang *et al.* 2016). Torrefaction has some effects on the chemical structure of cellulose (Zheng *et al.* 2015). During torrefaction, cellulose produces more C=O and C=C groups at 220 ℃ to 250 ℃ (Lv *et al.* 2012). In addition to organic matter, there is a certain amount of inorganic matter in biomass. The actual biomass torrefaction process is a complex thermochemical conversion system in which organic and inorganic components co-exist. However, there are only a small number of studies on the influence of active inorganic matter (*i.e.*, alkaline earth metals) in the torrefaction process on the torrefaction conversion route and mechanism.

Related research has confirmed the significant influence of alkaline earth metals (calcium and magnesium) on the thermochemical conversion process of organic matter (Yang *et al.* 2008). The effects of calcium and magnesium salts ($CaCl_2$ and $MgCl_2$) on the pyrolytic and catalytic characteristics of cellulose were investigated using a thermal gravimetric analyzer (Wang *et al.* 2015). The results of cellulose pyrolysis also indicated that decreases in temperature (between 150 ℃ and 400 ℃) promoted the formation of solid coke by alkaline earth metal chlorides ($MgCl_2$ and $CaCl_2$) (Shimada *et al.* 2008). Alkaline earth metals existing in biomass were usually in the form of free ions (Ca^{2+} and Mg^{2+}) and organic binding states (carboxylate) (Zhao *et al.* 2012). $Ca(CH_3COO)_2$ and $Mg(CH_3COO)_2$ played a catalytic role in cellulose decomposition (Wu *et al.* 2012). $Ca(OH)_2$ accelerated the hydrolysis of cellulose into glucose at 150 ℃ (Fang *et al.* 2011). Meanwhile, during the plant growth process, biomass absorbs a variety of alkaline earth metal salts. These metal salts are mainly present in the form of chlorides, hydroxides, and acetates (Pereira 1988; Szabó *et al.* 1996; Zevenhoven-Onderwater *et al.* 2001). Thus, in this article, chlorides ($CaCl_2$ and $MgCl_2$), hydroxides ($Ca(OH)_2$ and $Mg(OH)_2$), and acetates ($Ca(CH_3COO)_2$ and $Mg(CH_3COO)_2$), were selected as the model calcium and magnesium compounds. More detailed influencing rules of calcium and magnesium on solid products of cellulose torrefaction were studied. To reveal the influencing mechanism, the thermal gravimetric analysis (TGA) of torrefaction process was performed. The results were conducive to revealing the conversion mechanism of the biomass torrefaction process and provided some basic data and theoretical basis for the industrial application of torrefaction.

EXPERIMENTAL

Materials

Cellulose (microcrystalline, purity ≥ 99.2 wt%) was selected for this study. The calcium salts used as substitutes for calcium components in raw biomass were as follows: $CaCl_2$ (purity ≥ 96.0 wt%), $Ca(OH)_2$ (purity ≥ 95.0 wt%), and $Ca(CH_3COO)_2$ (purity ≥ 98.0 wt%). The magnesium salts used as substitutes were as follows: $MgCl_2$ (purity ≥ 98.0 wt%), $Mg(OH)_2$ (purity ≥ 95.0 wt%), and $Mg(CH_3COO)_2$ (purity≥99.0 wt%). All of the above materials, cellulose, calcium, and magnesium salts were purchased from the Sinopharm Chemical Reagent Company (Shanghai, China). Deionized water was supplied by the Nanjing Zhongdong Chemical Reagent Company (Nanjing, China). High purity nitrogen (purity ≥ 99.999 vol%) was purchased from the Nanjing Tianze Gas Company (Nanjing, China).

Sample preparation

According to the distribution characteristics of calcium and magnesium in actual biomass (Liao *et al.* 2004), in the current study, the calcium concentrations used were 0.5 wt%, 1 wt%, and 1.5 wt%; the magnesium concentrations were 0.3 wt%, 0.6 wt%, and 0.9 wt%. The impregnation method used in the feedstock preparation aimed to reveal the effects of calcium salts ($CaCl_2$, $Ca(OH)_2$, and $Ca(CH_3COO)_2$) and magnesium salts ($MgCl_2$, $Mg(OH)_2$, and $Mg(CH_3COO)_2$) on cellulose torrefaction. Regarding the impregnation method, 1 g of the cellulose and some calcium or magnesium salts were submerged in 20 mL of deionized water in a beaker. Then, these beakers were placed in a 25 ℃ water bath for 12 h. After the impregnation, the cellulose solution was immediately dried in an air-dry oven at 105 ℃ overnight until completely dehydrated (The control specimen (untreated cellulose) was not treated as above.).

Methods

Torrefaction apparatus and procedures

A schematic figure of the torrefaction apparatus is depicted in Fig. 1. The torrefaction experiments were conducted in a ceramic tubular reactor (length 600 mm, inner diameter 65 mm), which was heated by silicon carbide rods (5 kW). The cellulose and impregnated cellulose samples were placed in the porcelain boat and then placed into the center part of the tubular furnace. The tubular furnace was continuously injected with high purity nitrogen (N_2 flow rate, 50 mL/min). Then, the samples were heated to the holding temperature at a heating rate of 10 ℃/min and a residence time of 30 min. After the tubular furnace cooled to the room temperature, the solid products were removed and then placed in a dryer for Fourier transform infrared (FTIR) and X-ray diffraction (XRD) analyses.

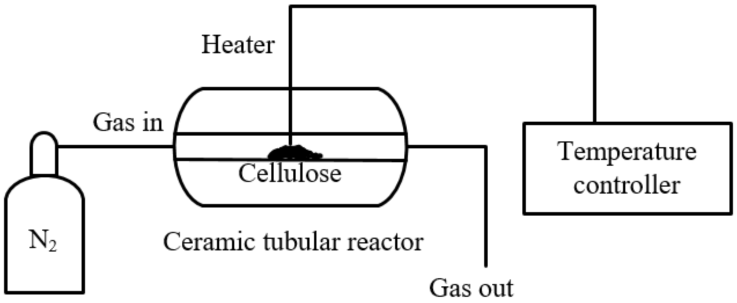

Fig. 1. The schematic figure of the torrefaction apparatus

The FTIR spectra were obtained using a FTIR spectrometer (Vertex 80v; Bruker Corporation, Karlsruhe, Germany) within the wavenumber range 500 cm^{-1} to 4000 cm^{-1} with a resolution of 4 cm^{-1} and 32 scans. X-ray diffractograms of cellulose and the solid products samples were taken using an X-ray diffractometer (Ultima IV; Rigaku Corporation, Tokyo, Japan) using Cu-Kα radiation at 40 kV and 40 mA in the scanning range of 5° to 60° at a scanning rate of 2°/min with a step of 0.02°. To investigate the kinetic process in the ceramic tubular reactor, the kinetic tests were further conducted using a thermogravimetric (TG) analyzer (STA409PC; Netzsch Corporation, Bavarian, Germany). The TG curve was acquired by heating the raw and impregnated cellulose samples from 30 ℃ to 300 ℃ at a constant heating rate of 10 ℃/min. A high-purity nitrogen gas flow of 50 mL/min was used as the purge gas to provide an inert atmosphere for the TG experiments.

RESULTS AND DISCUSSION

Solid Product Yield

The solid product yields of different calcium and magnesium salt cellulose samples torrefaction are shown in Figs. 2 and 3 (the definition of mass yield adopted in this paper was on dry ash free basis). Figures 2 and 3 show that with the increase of torrefaction temperature, the mass yields of the solid product dramatically decreased. Part of the cellulose began to decompose into some volatiles and was released from the solid phase at 200 ℃ to 300 ℃ (Zheng *et al.* 2015). Figures 2(a) and 3(a) show that at the torrefaction temperature of 200 ℃ to 275 ℃, the mass yields of calcium or magnesium-impregnated cellulose were lower than that of raw cellulose.

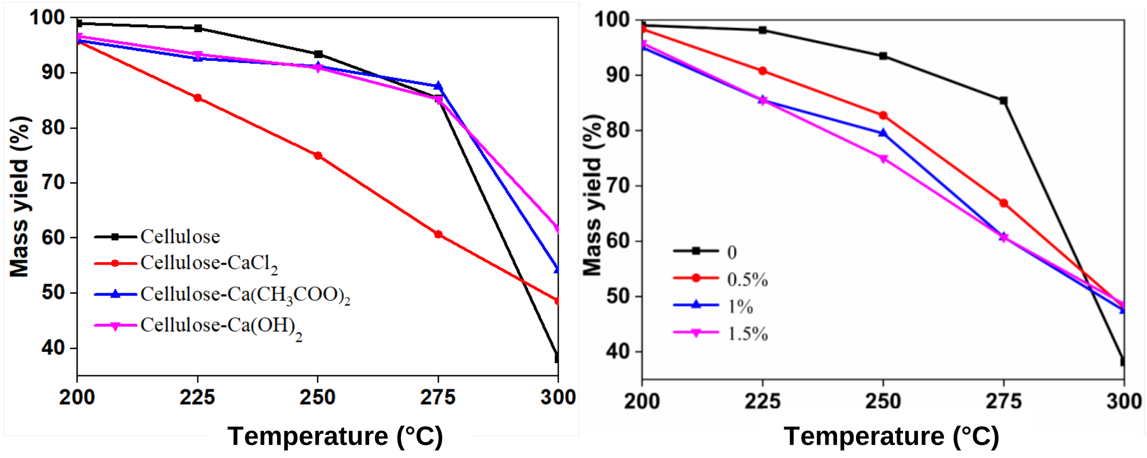

(a) 1.5% Ca **(b) CaCl₂**

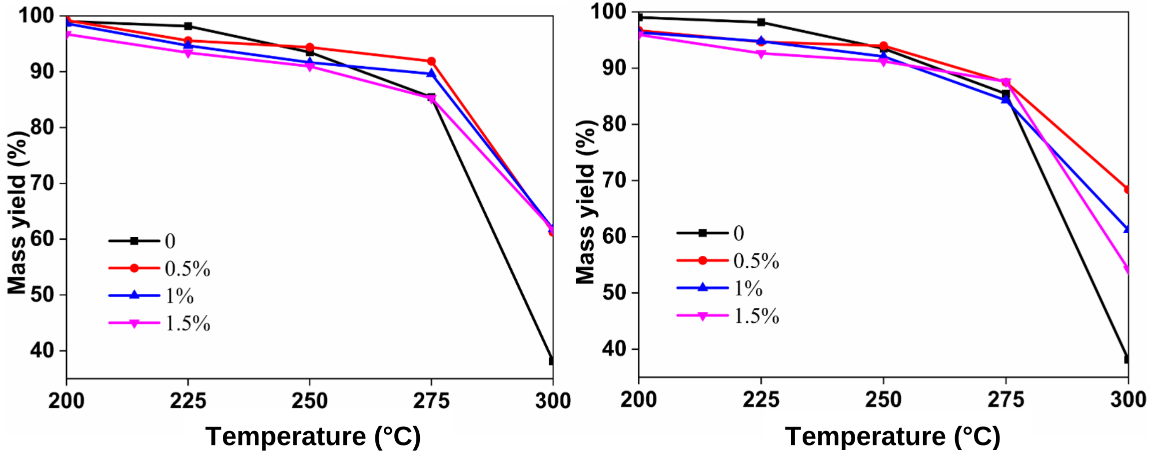

(c) Ca(OH)₂ **(d) Ca(CH₃COO)₂**

Fig. 2. Mass yields of solid products of calcium-impregnated cellulose torrefaction

At the higher temperature of 300 ℃, the mass yields of calcium or magnesium-impregnated cellulose were higher than that of raw cellulose. Wu *et al.* (2012) discovered that the raw cellulose began to pyrolyze at 290 °C, and cellulose with calcium or magnesium impregnation pyrolyzed at the low temperature of 210 °C. It can be inferred that calcium or magnesium had a strong catalytic effect on cellulose torrefaction. At 200 °C to 275 °C, calcium or magnesium salts promoted the cellulose decomposition process. At 300 °C, more char products were formed by hindering the release of volatiles and increasing secondary cracking reaction (Wu *et al.* 2012). Figure 2(a) shows that, compared to $Ca(OH)_2$ and $Ca(CH_3COO)_2$, $CaCl_2$ caused the mass yields of solid products at the torrefaction temperature of 200 °C to 275 °C to noticeably decrease. $CaCl_2$ had a stronger catalytic effect on cellulose torrefaction at 200 °C to 275 °C. Figures 2b and 2c show that the increase of $CaCl_2$ and $Ca(OH)_2$ concentrations had little effect on the solid product yields at 300 °C. However, in Fig. 2(d), the effects of $Ca(CH_3COO)_2$ concentration on mass yields were different. Figure 2(d) shows that the high $Ca(CH_3COO)_2$ concentration can decrease the mass yields, especially at 300 °C. During the torrefaction process, in theory, the decarboxylic reaction of $Ca(CH_3COO)_2$ can produce additional CO_2 and CH_4, and the higher $Ca(CH_3COO)_2$ concentration will produce more CO_2. As a result, the char in the torrefaction process may be reduced by the char consumption ($C + CO_2 \rightarrow 2CO$), especially at a high temperature of 300 °C (Reddy *et al.* 2014).

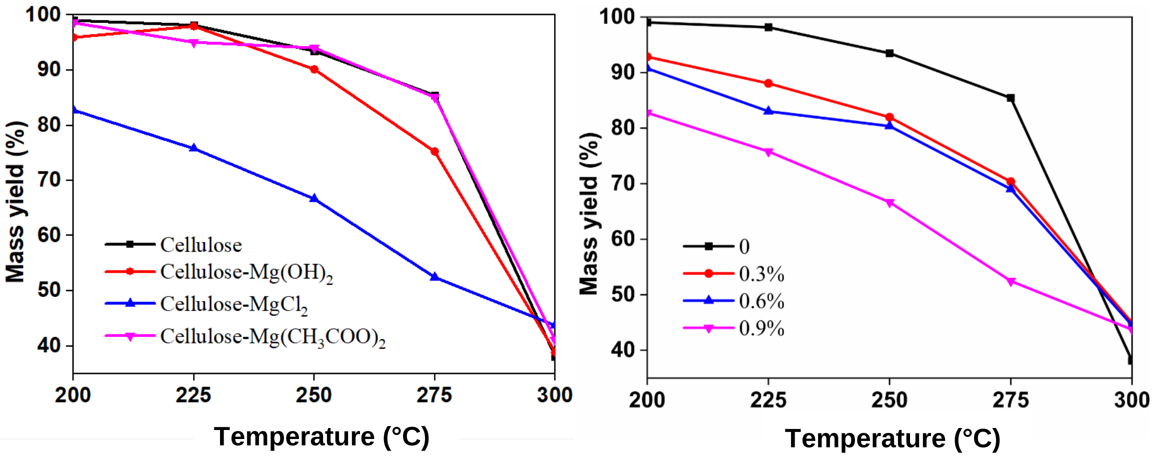

(a) 0.9% Mg

(b) $MgCl_2$

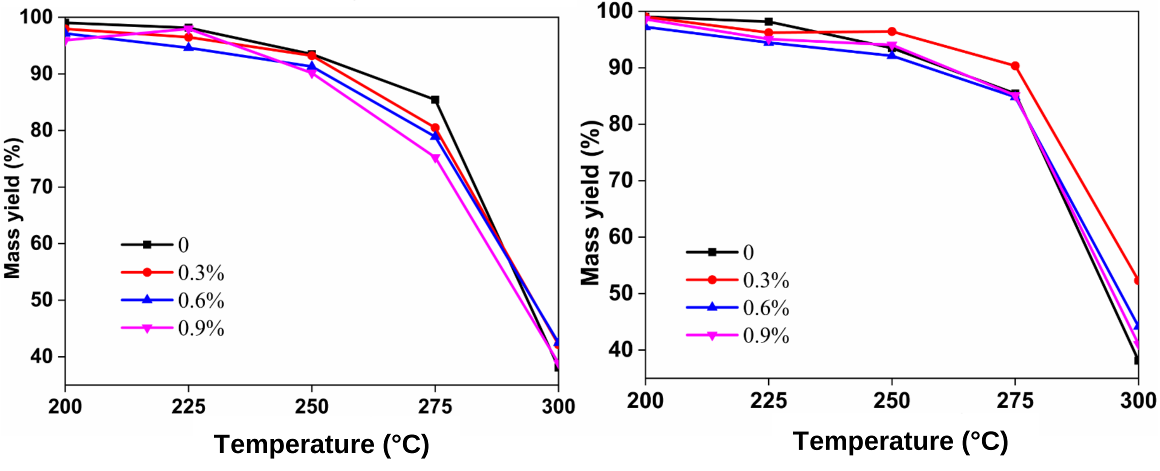

(c) $Mg(OH)_2$

(d) $Mg(CH_3COO)_2$

Fig. 3. Mass yields of solid products of magnesium-impregnated cellulose torrefaction

Figure 3(a) shows that compared to $Mg(OH)_2$ and $Mg(CH_3COO)_2$, $MgCl_2$ caused the mass yields of solid products to decrease in the range 200 °C to 275 °C, which was similar to the effect of $CaCl_2$. It can be concluded that alkali earth metal chloride salts ($CaCl_2$ and $MgCl_2$) promoted the cellulose decomposition process, especially at 200 °C to 275 °C. As shown in Figs. 3c and 3d, the changes of $Mg(OH)_2$ and $Mg(CH_3COO)_2$ concentrations had no obvious effect on the solid product yields. Wu *et al.* (2012) found that when the magnesium concentration was low (from 0.11 to 1.42 wt%), the catalytic effect on cellulose was weak. Because the changes in magnesium concentration were not obvious in Figs. 3c and 3d, the catalytic effects of magnesium on solid products were almost the same. However, Wu *et al.* (2012) also discovered that the catalytic ability of chloride metals was susceptible to the concentration. Moreover, Wang *et al.* (2015) discovered that with the increase of $MgCl_2$ concentration from 0 to 10 wt%, the maximum pyrolysis weight loss rate of cellulose decreased regularly from 2.1%/°C to 1.4%/°C. The addition of $MgCl_2$ promoted the catalytic pyrolysis of cellulose. It likely led to the decrease in the mass yield of solid product with the increase of $MgCl_2$ concentration. Therefore, in Fig. 3(b), with the increase of $MgCl_2$ concentration at 200 °C to 275 °C, the inhibition effect of $MgCl_2$ on the mass yield of solid product was enhanced.

FTIR Analysis

Within the range of 200 °C to 300 °C, the high torrefaction temperature of 300 °C had more noticeable effects on cellulose. The FTIR spectra of raw and calcium or magnesium-impregnated cellulose torrefaction at 300 °C are shown in Fig. 4.

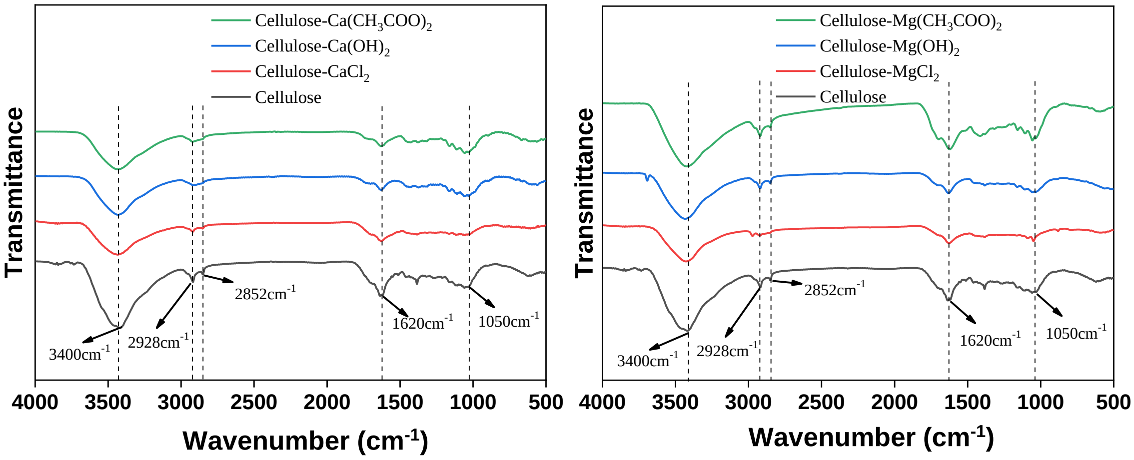

(a) 1.5% Ca **(b) 0.9% Mg**

Fig. 4. FTIR spectra of solid products (raw and calcium- or magnesium-impregnated cellulose torrefaction at 300 °C)

In Fig. 4, the spectrum shapes of torrefied cellulose with calcium or magnesium impregnation were similar to that of torrefied raw cellulose, while the intensity peaks were slightly different. Figure 4 shows that the polysaccharide characteristics of cellulose were retained, and the whole structures were not fundamentally changed. In Fig. 4, the absorbances at wavenumbers of 3400 cm^{-1}, 2928 cm^{-1}, 2852 cm^{-1}, 1620 cm^{-1}, and 1050 cm^{-1} are predominately related to the O–H stretch vibrations of hydrogen bonded hydroxyl groups or absorbed water, CH_3 asymmetric, CH_2 symmetric stretch vibration, O–H bending mode of absorbed/crystal water, and C–O vibration, respectively (Sun *et al.* 2010). Their intensity decreased with calcium or magnesium-impregnated cellulose. The results can be explained by depolymerization, ring breakage, fragmentation, and serious polycondensation at this holding torrefaction temperature (Zheng *et al*. 2015). It meant that calcium or magnesium had a catalytic effect on the above reactions during torrefaction. In addition, Fig. 4 shows that the spectrum shapes of torrefied cellulose with calcium impregnation were similar to that of torrefied cellulose with magnesium impregnation. Wu *et al.* (2012) found the catalytic effects on cellulose pyrolysis were in the order of potassium > sodium > magnesium or calcium. This meant that calcium and magnesium had almost the same catalytic effect on cellulose during torrefaction. In Fig. 4(a), the intensity of wavenumber between 500 cm^{-1} and 1620 cm^{-1} of $CaCl_2$ decreased greatly, which showed that $CaCl_2$ had a stronger effect than other calcium salts. In Fig. 4(b), the intensity of the wavenumber between 500 cm^{-1} and 4000 cm^{-1} of $Mg(CH_3COO)_2$ was similar to that of torrefied raw-cellulose. Thus, it can be concluded that $Mg(CH_3COO)_2$ had less of an effect than other magnesium salts.

XRD Analysis

Cellulose is a linear homopolymer composed of cellobiose, which consists of crystalline and amorphous structures. The crystalline cellulose had a higher cohesive energy density than amorphous cellulose, which is consistent with an expectation that crystalline cellulose was much more thermally stable (Mazeau and Heux 2008). Therefore, it was important to study the variation in cellulose crystallinity during torrefaction. The XRD analysis of the solid products of calcium or magnesium salt-impregnated cellulose torrefaction are presented in Fig. 5.

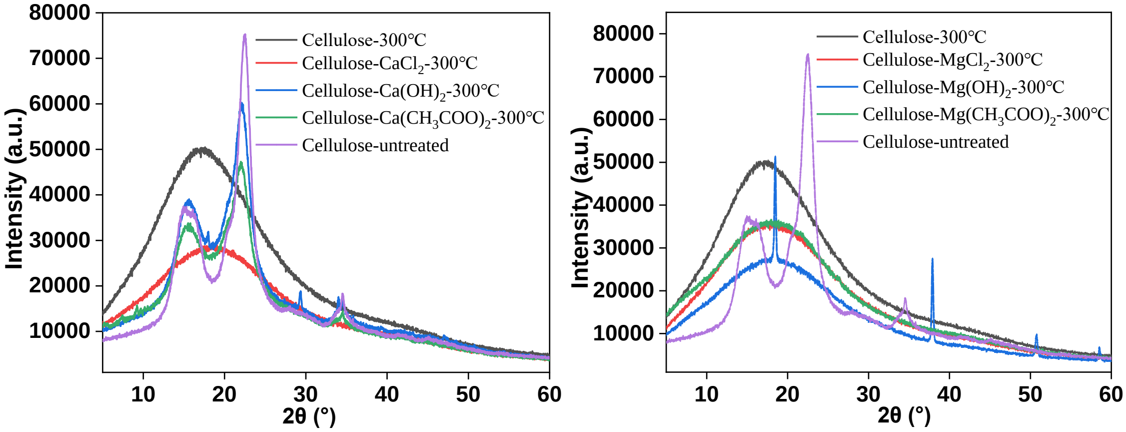

(a) 1.5% Ca **(b) 0.9% Mg**

Fig. 5. XRD patterns of solid products (raw and calcium- or magnesium-impregnated cellulose torrefaction at 300 °C)

Commonly, the characteristic signal peak of crystalline cellulose is the crystalline plane -002 at $2\theta = 22.6°$ (Wang *et al.* 2017b). In Fig. 5(a), the characteristic signal peak of torrefied cellulose was at $2\theta = 17.2°$, and the characteristic signal peaks of torrefied $CaCl_2$, $Ca(OH)_2$, and $Ca(CH_3COO)_2$-impregnated cellulose were at $2\theta = 17.6°$, 15.7°, and 15.6°, respectively. Table 1 shows that the crystallinity of the torrefied cellulose changed with impregnating calcium salts. The crystallinity of torrefied $CaCl_2$, $Ca(OH)_2$, and

$Ca(CH_3COO)_2$-impregnated cellulose decreased to 7.66%, 34.80%, and 28.57%. This showed that $CaCl_2$ had a stronger effect than other calcium salts. In Fig. 5(a), the figures of torrefied cellulose (cellulose-$Ca(OH)_2$ and cellulose-$Ca(CH_3COO)_2$) were close to that of untreated cellulose, this implied that $Ca(OH)_2$ and $Ca(CH_3COO)_2$ tended to maintain the crystalline structure of the cellulose during the torrefaction. And the signal peak at 2θ = 29.32° was attributed to $Mg(OH)_2$ solid products (Giorgi *et al.* 2005). It was likely that Mg^+ had turned into $Mg(OH)_2$ solid products at the temperature of 300 ℃ (Giauque and Archibald 1937). In Fig. 5(b), the characteristic signal peaks of $MgCl_2$, $Mg(OH)_2$, and $Mg(CH_3COO)_2$ salts impregnated cellulose were at 2θ = 18.4°, 18.5°, and 16.2°. In Table 2, it also shown that the crystallinity of the torrefied sample impregnated with magnesium was greatly reduced. The crystallinity of torrefied $MgCl_2$, $Mg(OH)_2$, and $Mg(CH_3COO)_2$-impregnated cellulose decreased to 9.22%, 13.55%, and 12.03%, which meant that $MgCl_2$ had a stronger catalytic effect on cellulose during torrefaction. In Fig. 5(b), the four signal peaks at 2θ = 18.52°, 37.98°, 50.78°, and 58.66° were attributed to $Mg(OH)_2$ solid products (Giorgi *et al.* 2005). It was just like cellulose-$Ca(OH)_2$, Mg^+ had turned into $Mg(OH)_2$ solid products at 300 ℃ during torrefaction (Giauque and Archibald 1937).

Table 1. Crystallinity Index (CrI) of Solid Products by Torrefaction Using XRD

Samples	CrI (%)
Cellulose	51.13
Cellulose-$CaCl_2$	7.66
Cellulose-$Ca(OH)_2$	34.80
Cellulose-$Ca(CH_3COO)_2$	28.57

Holding temperature: 300 °C; calcium concentration: 1.5%

Table 2. CrI of Solid Products by Torrefaction Using XRD

Samples	CrI (%)
Cellulose	51.13
Cellulose-$MgCl_2$	9.22
Cellulose-$Mg(OH)_2$	13.55
Cellulose-$Mg(CH_3COO)_2$	12.03

Holding temperature: 300 °C; magnesium concentration: 0.9%

TGA Analysis

The TG/ derivative thermogravimetry (DTG) curves of calcium or magnesium salt-impregnated cellulose torrefaction process obtained from the TGA experiments are shown in Figs. 6 and 7. As shown, as the torrefaction temperature increased from 200 ℃ to 300 ℃, the mass and the mass loss rate of samples dramatically decreased. Yu *et al.* (2017) discovered crystalline cellulose degrades into an amorphous form during torrefaction, which results in weaker thermal stability. In Fig. 6(a), compared to the raw cellulose, the calcium-rich samples (raw cellulose and impregnated samples) exhibited a higher percentage loss and rate in the mass, especially $CaCl_2$. Leng *et al.* (2019) thought $CaCl_2$ promoted the decomposition of cellulose into a non-solid phase product during the torrefaction process. It meant that with the increase of torrefaction temperature, the solid yields of $CaCl_2$ gradually decreased. As shown in Fig. 6(b), compared to $Ca(OH)_2$ and $Ca(CH_3COO)_2$, the mass lose rate of $CaCl_2$-impregnated cellulose decreased from 210 ℃ to 260 ℃. $CaCl_2$ was shown to have a stronger catalytic effect on cellulose torrefaction. In Fig. 7, compared to the $Mg(OH)_2$- and $Mg(CH_3COO)_2$-impregnated cellulose, $MgCl_2$-

impregnated cellulose decreased dramatically. Wang *et al.* (2015) found that $MgCl_2$ greatly promoted the catalytic pyrolysis of cellulose. This meant that with the addition of $MgCl_2$, the solid yields of $CaCl_2$ gradually decreased. In Fig. 7(b), it can be seen that compared to $Mg(OH)_2$ and $Mg(CH_3COO)_2$, the mass loss rate of $MgCl_2$-impregnated cellulose decreased from 177 °C to 224 °C. This meant that $MgCl_2$ had a stronger catalytic effect on cellulose during torrefaction. The TGA torrefaction processes of calcium or magnesium salts-impregnated cellulose torrefaction process were continuous from 30 °C to 300 °C, with no residence time. However, in the "Solid product yield" section, raw cellulose and calcium- or magnesium-impregnated cellulose samples were heated to the holding temperature at the heating rate of 10 °C/min, with a residence time of 30 min. Thus, the definition of mass loss in TG was different from that of the "Solid product yield" section.

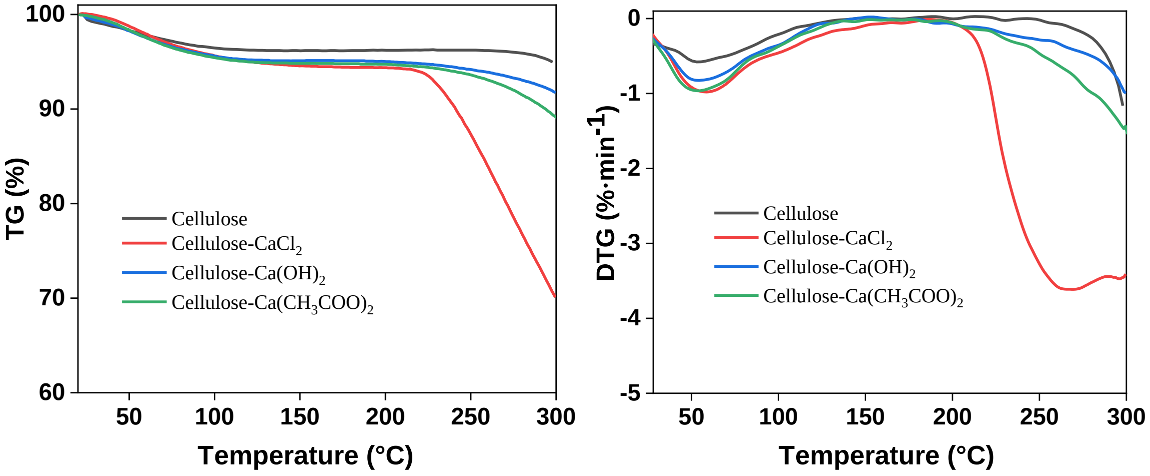

(a) TG (1.5% Ca) **(b) DTG (1.5% Ca)**

Fig. 6. Torrefaction process using TGA (1.5% Ca)

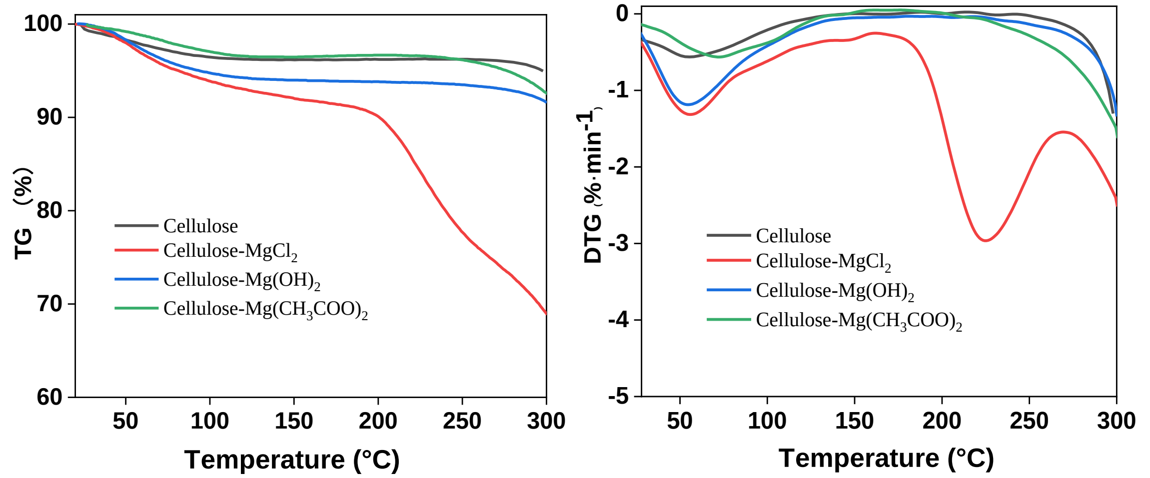

(a) TG (0.9% Mg) **(b) DTG (0.9% Mg)**

Fig. 7. Torrefaction process using TGA (0.9% Mg)

To have a better understanding of torrefaction effects on raw cellulose and calcium- or magnesium salts-impregnated cellulose samples, based on the classical kinetic formulas (Eqs. 1 to 3) (Ren *et al.* 2013; Zhou *et al.* 2017), the corresponding kinetic analysis was conducted. Equations 1 to 3 are as follows:

$$\frac{\mathrm{d}\alpha}{\mathrm{d}t} = k(1-\alpha)^n \tag{1}$$

$$k = Ae^{-\frac{E}{\mathrm{R}T}} \tag{2}$$

$$\ln\left[-\frac{\ln(1-\alpha)}{T^2}\right] = \ln\frac{A\mathrm{R}}{E\beta} - \frac{E}{\mathrm{R}T} \tag{3}$$

Based on the Arrhenius law, k (reaction rate constant) can be defined as shown in Eq. 2. The simulation of the cellulose torrefaction process usually has been based on the assumption of a first-order (n = 1) reaction (Ren *et al.* 2013). Through using the kinetic parametric solution of Coats-Redfern (Ganeshan *et al.* 2017), Eq. 2 can be expressed as Eq. 3, where α is the mass loss rate of cellulose (%), β is heating rate value (10 K/min), t is holding time (min), k is reaction rate constant (min^{-1}), R is the gas constant ($\mathrm{J{\cdot}mol^{-1}{\cdot}K^{-1}}$), E (activation energy, $\mathrm{kJ{\cdot}mol^{-1}}$) is the minimum amount of energy required to convert a normal stable molecule into a reactive molecule, and A (pre-exponential factor, min^{-1}) is an empirical relationship between temperature and rate coefficient. Therefore, E and A in Tables 3 and 4 are considered as two crucial kinetics parameters to evaluate the torrefaction process of raw and calcium or magnesium salts-impregnated cellulose samples. The R^2 (coefficient of determination) is close to 1; thus, it can be inferred that the values of E and A are close to that of the real torrefaction process. Tables 3 and 4 show that calcium or magnesium chloride can greatly reduce the activation energy of cellulose torrefaction.

Table 3. Kinetic Parameters of the Sample Torrefaction (1.5 wt% Ca)

Samples	E ($\mathrm{kJ{\cdot}mol^{-1}}$)	A (min^{-1})	R^2 (Coefficient of Determination)
Cellulose	162.05	2.96×10^{14}	0.9765
Cellulose-$CaCl_2$	78.13	1.02×10^{15}	0.9638
Cellulose-$Ca(OH)_2$	78.09	1.27×10^{15}	0.9669
Cellulose-$Ca(CH_3COO)_2$	77.90	1.06×10^{15}	0.9421

Table 4. Kinetic Parameters of the Sample Torrefaction (0.9 wt% Mg)

Samples	E ($\mathrm{kJ{\cdot}mol^{-1}}$)	A (min^{-1})	R^2 (Coefficient of Determination)
Cellulose	162.05	2.96×10^{14}	0.9765
Cellulose-$MgCl_2$	57.25	1.20×10^{13}	0.9864
Cellulose-$Mg(OH)_2$	90.46	2.08×10^{16}	0.9363
Cellulose-$Mg(CH_3COO)_2$	99.66	1.26×10^{17}	0.9421

Tables 3 and 4 show that the activation energy of raw cellulose was 162.0 kJ·mol^{-1}. In Table 3, the activation energy of calcium salts-impregnated cellulose decreased to 78.1 kJ·mol^{-1} ($CaCl_2$), 78.1 kJ·mol^{-1} ($Ca(OH)_2$), and 77.9 kJ·mol^{-1} ($Ca(CH_3COO)_2$). The calcium salts had a strong catalytic effect on cellulose torrefaction. In Table 4, the activation energy of magnesium salts-impregnated cellulose decreased to 57.2 kJ·mol^{-1} ($MgCl_2$), 90.5 kJ·mol^{-1} ($Mg(OH)_2$), and 99.7 kJ·mol^{-1} ($Mg(CH_3COO)_2$). It showed that magnesium salts also had a strong catalytic effect on cellulose torrefaction, especially $MgCl_2$.

CONCLUSIONS

1. The alkaline earth chlorides had the biggest effects on cellulose torrefaction. The solid product yield of calcium- or magnesium salts-impregnated cellulose torrefaction was lower than that of raw cellulose torrefaction at 200 ℃ to 275 ℃. This meant that calcium or magnesium had a strong catalytic effect on cellulose decomposition. However, the calcium- or magnesium salts-impregnated cellulose had higher solid yields than raw cellulose at the torrefaction temperature of 300 ℃. More char products were formed by hindering the release of volatiles and increasing secondary cracking reaction at 300 ℃.
2. During the torrefaction process, calcium or magnesium had a catalytic effect on depolymerization, ring breakage, fragmentation, and serious polycondensation of cellulose. The characteristic signal peaks of cellulose ($2\theta = 22.6°$) changed. The crystallinity of the torrefied cellulose with impregnated calcium or magnesium salts decreased from 51.1% (raw cellulose) to 7.7% ($CaCl_2$), 34.8% ($Ca(OH)_2$), 28.6% ($Ca(CH_3COO)_2$), 9.2% ($MgCl_2$), 13.6% ($Mg(OH)_2$), and 12.0% ($Mg(CH_3COO)_2$). This implied that $CaCl_2$ and $MgCl_2$ had a stronger effect than other calcium or magnesium salts. It is likely that Mg^+ turned into $Mg(OH)_2$ solid products at the temperature of 300 ℃.
3. The impregnated calcium or magnesium salts reduced the activation energy of torrefaction (raw cellulose: 162.0 kJ·mol^{-1}) to 78.1 kJ·mol^{-1} ($CaCl_2$), 78.1 kJ·mol^{-1} ($Ca(OH)_2$), 77.9 kJ·mol^{-1} ($Ca(CH_3COO)_2$), 57.2 kJ·mol^{-1} ($MgCl_2$), 90.5 kJ·mol^{-1} ($Mg(OH)_2$), and 99.7 kJ·mol^{-1} ($Mg(CH_3COO)_2$). It meant that calcium or magnesium salts (especially $MgCl_2$) had a strong catalytic effect on cellulose torrefaction

ACKNOWLEDGEMENTS

The research was financially supported by the National Natural Science Foundation of China (No. 51606103), the Opening Research Fund Program of Key Laboratory of Energy Thermal Conversion and Control of Ministry of Education of Southeast University (No. 2016007), and the Practice Innovation Training Program for College Students in Jiangsu Province (201910298003Y). The authors acknowledge the support of Advanced Analysis and Testing Center of Nanjing Forestry University.

REFERENCES CITED

Chen, D. Y., Zhou, J. B., and Qiang, L. (2014). "Upgrading of rice husk by torrefaction and its influence on the fuel properties," *BioResources* 9(4), 5893-5905. DOI: 10.15376/biores.9.4.5893-5905

Fang, Z., Zhang, F., Zeng, H.-Y., and Guo, F. (2011). "Production of glucose by hydrolysis of cellulose at 423K in the presence of activated hydrotalcite nanoparticles," *Bioresource Technology* 102(17), 8017-8021. DOI: 10.1016/j.biortech.2011.06.052

Ganeshan, G., Shadangi, K. P., and Mohanty, K. (2017). "Degradation kinetic study of pyrolysis and co-pyrolysis of biomass with polyethylene terephthalate (PET) using *Coats–Redfern* method," *Journal of Thermal Analysis and Calorimetry* 131(2), 1803-1816. DOI: 10.1007/s10973-017-6597-5

Giauque, W. F., and Archibald, R. C. (1937). "The entropy of water from the third law of thermodynamics. The dissociation pressure and calorimetric heat of the reaction $Mg(OH)_2$=MgO+H_2O. The heat capacities of $Mg(OH)_2$ and MgO from 20 to 300°K," *Journal of the American Chemical Society* 59(3), 561-569. DOI: 10.1021/ja01282a039

Giorgi, R., Bozzi, C., Dei, L., Gabbiani, C., Ninham, B. W., and Baglioni, P. (2005). "Nanoparticles of $Mg(OH)_2$: Synthesis and application to paper conservation," *Langmuir* 21(18), 8495-8501. DOI: 10.1021/la050564m

Huang, Y., Gao, Y. X., Zhou, H., Sun, H. Q., Zhou, J. B., and Zhang, S. (2019). "Pyrolysis of palm kernel shell with internal recycling of heavy oil," *Bioresource Technology* 272, 77-82. DOI: 10.1016/j.biortech.2018.10.006

Leng, E., Costa, M., Gong, X., Zheng, A., Liu, S., and Xu, M. H. (2019). "Effects of KCl and $CaCl_2$ on the evolution of anhydro sugars in reaction intermediates during cellulose fast pyrolysis," *Fuel* 251, 307-315. DOI: 10.1016/j.fuel.2019.04.006

Liao, C.-P., Wu, C.-Z., Yan, Y.-G., and Huang, H.-T. (2004). "Chemical elemental characteristics of biomass fuels in China," *Biomass and Bioenergy* 27(2), 119-130. DOI: 10.1016/j.biombioe.2004.01.002

Liu, S. S., Wu, Y. S., Zhang, J., Gao, W. R., Zhou, J. B., Huang, Y., Zhang, S., and Zhang, H. (2019). "Volatile-char interactions during biomass pyrolysis: A case study of a lignin model compound and functionalized graphitized carbon nanotubes," *Energy & Fuels* 33(11), 11339-11345. DOI: 10.1021/acs.energyfuels.9b03247

Lv, P., Almeida, G., and Perré, P. (2012). "Torrefaction of cellulose: Validity and limitation of the temperature/duration equivalence," *BioResources* 7(3), 3720-3731. DOI: 10.15376/biores.7.3.3720-3731

Mazeau, K., and Heux, L. (2008). "Molecular dynamics simulations of bulk native crystalline and amorphous structures of cellulose," *Journal of Physical Chemistry B* 107(10), 2394-2403. DOI: 10.1021/jp0219395

Mohan, D., Pittman, C. U., and Steele, P. H. (2006). "Pyrolysis of wood/biomass for bio-oil: A critical review," *Energy & Fuels* 20(3), 848-889. DOI: 10.1021/ef0502397

Pereira, H. (1988). "Variability in the chemical composition of plantation eucalypts (*Eucalyptus globulus* Labill.)," *Wood & Fiber Science* 20(1), 82-90.

Reddy, S. N., Nanda, S., Dalai, A. K., and Kozinski, J. A. (2014). "Supercritical water gasification of biomass for hydrogen production," *Internation Journal of Hydrogen Energy* 39(13), 6912-6926. DOI: 10.1016/j.ijhydene.2014.02.125

Ren, S., Lei, H., Wang, L., Bu, Q., Chen, S., and Wu, J. (2013). "Thermal behaviour and kinetic study for woody biomass torrefaction and torrefied biomass pyrolysis by TGA," *Biosystems Engineering* 116(4), 420-426. DOI: 10.1016/j.biosystemseng.2013.10.003

Rousset, P., Aguiar, C., Vholle, G., Anacleto, J., and Souza, M. D. (2013). "Torrefaction of babassu: A potential utilization pathway," *BioResources* 8(1), 358-370. DOI: 10.15376/biores.8.1.358-370

Saidur, R., Abdelaziz, E. A., Demirbas, A., Hossain, M. S., and Mekhilef, S. (2011). "A review on biomass as a fuel for boilers," *Renewable and Sustainable Energy Reviews* 15(5), 2262-2289. DOI: 10.1016/j.rser.2011.02.015

Shimada, N., Kawamoto, H., and Saka, S. (2008). "Different action of alkali/alkaline earth metal chlorides on cellulose pyrolysis," *Journal of Analytical and Applied Pyrolysis* 81(1), 80-87. DOI: 10.1016/j.jaap.2007.09.005

Sun, Q. F., Yu, H. P., Liu, Y., Li, J., Cui, Y., and Lu, Y. (2010). "Prolonging the combustion duration of wood by TiO_2 coating synthesized using cosolvent-controlled hydrothermal method," *Journal of Materials Science* 45(24), 6661-6667. DOI: 10.1007/s10853-010-4758-z

Szabó, P., Várhegyi, G., Till, F., and Faix, O. (1996). "Thermogravimetric/mass spectrometric characterization of two energy crops, *Arundo donax* and *Miscanthus sinensis*," *Journal of Analytical and Applied Pyrolysis* 36(2), 179-190. DOI: 10.1016/0165-2370(96)00931-X

Wang, C., Bai, L. J., and Yan, C. X. (2015). "Effect of metallic salts of potassium, calcium and magnesium on biomass pyrolysis," *Journal of Tianjin University of Science & Technology* 30(2), 33-42. DOI: 10.13364/j.issn.1672-6510.20140092

Wang, S. R., Dai, G. X., Ru, B., Wang, X., Xiao, G., and Luo, Z. Y. (2016). "Influence of torrefaction on the characteristics and pyrolysis behavior of cellulose," *Energy* 120, 864-871. DOI:10.1016/j.energy.2016.11.135

Wang, S. R., Dai, G. X., Haiping, Y., and Luo, Z. Y. (2017a). "Lignocellulosic biomass pyrolysis mechanism: A state-of-the-art review," *Process in Energy and Combustion Science* 62, 33-86. DOI:10.1016/j.pecs.2017.05.004

Wang, S. R., Dai, G. X., Ru, B., Zhao, Y., Wang, X., Xiao, G., and Luo, Z. Y. (2017b). "Influence of torrefaction on the characteristics and pyrolysis behavior of cellulose," *Energy* 120, 864-871. DOI: 10.1016/j.energy.2016.11.135

Wu, H. X., Zhao, Z. L., Zhang, W., Li, H., and He, F. (2012). "Effects of alkali/alkaline earth metals on pyrolysis characteristics of cellulose," *Transactions of the CSAE* 28(4), 215-220. DOI: 10.3969/j.issn.1002-6819.2012.04.036

Yang, T., Hu, S., and Chen, Q. Q. (2008). "Review on characteristics and detection technology of the alkali/alkaline earth metal during biomass thermal utilization," *Biomass Chemical Engineering* 42(6), 49-54. DOI: 10.3969/j.issn.1673-5854.2008.06.011

Yu, J., Paterson, N., Blamey, J., and Millan, M. (2017). "Cellulose, xylan and lignin interactions during pyrolysis of lignocellulosic biomass," *Fuel* 191, 140-149. DOI: 10.1016/j.fuel.2016.11.057

Zevenhoven-Onderwater, M., Backman, R., Skrifvars, B.-J., and Hupa, M. (2001). "The ash chemistry in fluidised bed gasification of biomass fuels. Part I: Predicting the chemistry of melting ashes and ash–bed material interaction," *Fuel* 80(10), 1489-1502. DOI: 10.1016/S0016-2361(01)00026-6

Zhao, L., Zhang, J., and Ding, Q. Z. (2012). “Dissolution characteristics of inorganic elements existing in biomass during the supercritical water gasification process,” *Energy Sources, Part A: Recovery Utilization and Environmental Effects* 34(20), 1893-1900. DOI: 10.1080/15567036.2011.592913

Zhao, C., Qiao, X. L., Cao, Y., and Shao, Q. J. (2017). “Application of hydrogen peroxide presoaking prior to ammonia fiber expansion pretreatment of energy crops,” *Fuel* 205, 184-191. DOI: 10.1016/j.fuel.2017.05.073

Zheng, A. Q., Jiang, L. Q., Huang, Z., Zhao, K., Wei, G., Wang, X., He, F., and Li, H. B. (2015). “Impact of torrefaction on chemical structure and catalytic fast pyrolysis behavior of hemicellulose, lignin and cellulose,” *Energy & Fuels* 29(12), 8027-8034. DOI: 10.1021/acs.energyfuels.5b01765

Zhou, L. M., Zou, H. B., Wang, Y., Le, Z., Liu, Z., and Adesina, A. A. (2017). “Effect of potassium on thermogravimetric behavior and co-pyrolytic kinetics of wood biomass and low density polyethylene,” *Renewable Energy* 102(Part A), 134-141. DOI: 10.1016/j.renene.2016.10.028

Article submitted: October 19, 2019; Peer review completed: December 31, 2019; Revised version received: January 16, 2020; Accepted: January 18, 2020; Published: January 22, 2020.
DOI: 10.15376/biores.15.1.1678-1691